Indium-Tin-Oxide Nanowhiskers Crystalline Silicon Photovoltaics Combining Micro- and Nano-Scale Surface Textures

C.H. Chang[a], M. H. Hsu[a], W. L. Chang[b], and W. C. Sun[b], and Peichen Yu[a]*
[a]Department of Photonics and Institute of Electro-Optical Engineering,National Chiao Tung University, Hsinchu 30050, Taiwan;
[b]Green Energy & Environment Research Labs, Industrial Technology Research Institute, , 195, Sec. 4, Chung Hsing Road, Chutung, Hsinchu, 310 Taiwan, R.O.C.

ABSTRACT

In this work, we present a solution that employs combined micro- and nano-scale surface textures to increase light harvesting in the near infrared for crystalline silicon photovoltaics, and discuss the associated antireflection and scattering mechanisms. The combined surface textures are achieved by uniformly depositing a layer of indium-tin-oxide nanowhiskers on passivated, micro-grooved silicon solar cells using electron-beam evaporation. The nanowhiskers facilitate optical transmission in the near-infrared, which is optically equivalent to a stack of two dielectric thin-films with step- and graded- refractive index profiles. The ITO nanowhiskers provide broadband anti-reflective properties (R<5%) in the wavelength range of 350-1100nm. In comparison with conventional Si solar cell, the combined surface texture solar cell shows higher external quantum efficiency (EQE) in the range of 700-1100nm. Moreover, the ITO nano-whisker coating Si solar cell shows a high total efficiency increase of 1.1% (from 16.08% to17.18%). Furthermore, the nanowhiskers also provide strong forward scattering for ultraviolet and visible light, favorable in thin-wafer silicon photovoltaics to increase the optical absorption path.

Keywords: photovoltaics, indium-tin-oxide, nanostructure

1. INTRODUCTION

Anti-reflective coating (ARC) minimizes the reflectance loss of solar cell for the broadband solar spectra and varying incident angles [1-3]. The conventional anti-reflective coatings are in general realized by a stack of thin film dielectric layers, which only improve light harvesting in a relatively narrow spectrum response and at a specific incident angle. In the last decade, versatile sub-wavelength structures (SWS) demonstrate broadband wavelength region and omnidirectional antireflective properties, such as biomimetic moth-eye structure [4-8] and random nano-rods [9-11]. However, the high fabrication cost, involving either electron beam (e-beam) lithography and/or dry etching, becomes technical barrier to apply to silicon solar cells. Moreover, the fabrication process should also avoid generating recombination defects on the surface, which deteriorates the device performance. Therefore, growth-up fabrication methods of SWS ARC in commercial solar cells are better and more realistic than etching methods.

Recently, the porous thin film of ITO nanorods, prepared by oblique-angle deposition, function as a low-refractive index layer of the omnidirectional reflector on light-emitting diodes. Moreover, the ITO nano-collumns, prepared by the oblique-angle deposition with an incident nitrogen flux, offer broadband antireflective properties on GaAs solar cell due to the graded refractive index profile [12-13]. Herein, we integrate an ITO nanowhisker layer on a reference micro-textured crystalline silicon solar cell, passivated by an 80-nm-thick SiNx layer. The ITO nanowhisker cell shows superior omnidirectional and broadband wavelength range antireflective properties to the reference cell. The external quantum efficiency (EQE) measurement confirms the fact that the enhancement in near-infrared is a result of reflection reduction by ITO nanowhisker. As a result, the power conversion efficiency (PCE) of the cell with ITO-nanowhisker ARC achieves 17.18%, compared to 16.08% for the reference cell. Angular-resolved reflectance spectroscopy shows that the ITO nanowhisker silicon cell exhibits broadband antireflective characteristics (R < 7%) in the wavelength range from 500 nm to 1000nm, up to an incident angle of 70 degree. Furthermore, the angular-resolved short-circuit current result reveals that the ITO nanowhisker solar cell has higher absorption for wide incident angles.

Physics and Simulation of Optoelectronic Devices XIX, edited by Bernd Witzigmann, Fritz Henneberger, Yasuhiko Arakawa, Alexandre Freundlich, Proc. of SPIE Vol. 7933, 79332M · © 2011 SPIE · CCC code: 0277-786X/11/$18 · doi: 10.1117/12.876853

2. EXPERIMENTAL

The ITO nanowhiskers were deposited using an electron-beam evaporation system by introducing 1 sccm nitrogen. The composition of the ITO target was 95% In_2O_3+ 5% SnO_2. The chamber pressure was controlled at 10^{-4} torr and the substrate temperature was controlled at 260℃. The ITO nanowhiskers were grown by self-catalytic vapor-liquid-solid mechanism. Because the chamber was lacking of oxygen in the process, the Sn atom would function as catalyst in the In-Sn-O ternary phase and form a liquid phase on the surface [14-15]. The In_2O_3 crystal would nuclei crystal cores in the liquid shell and grow-up the whisker structure, and the surface would exist high Sn composition as the catalyst layer [16-17].

Firstly, the device fabrication followed standard Si solar cell processes, including the KOH solution etching, $POCl_3$ diffusion, 80nm thick SiNx passivation layer depositing, front and back contact screen-printing process, without the co-firing step. The cell area is 2.5x3.5 cm^2. Secondly, the all cells were separated into two groups for the reference cells and the process cells. The ITO nanowhiskers were deposited on the process cell, as the ITO nanowhisker cell. Therefore, the ITO nanowhisker cell could combined the nano- and micro- structure as the complex ARC layer, compared to the micro-structure reference cell. Finally, the ITO nanowhisker cells and reference cells were co-fired to optimize the cell efficiency.

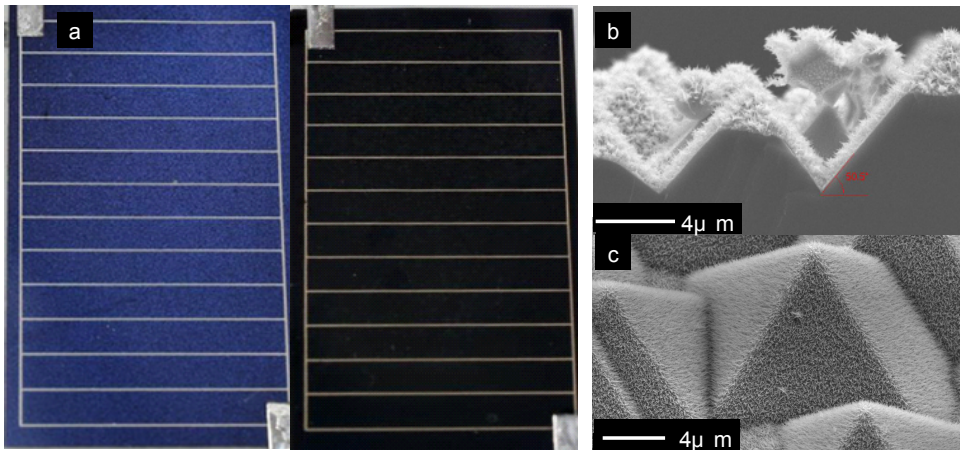

Figure 1 (a) The photograph of fabricated cells with the conventional SiNx ARC on the left and the nano-whisker ARC on the right (b) The cross-sectional SEM image of the ITO nano-whiskers deposited on textured Si solar cells, and (c) the SEM image of the top view.

The photographs of fabricated solar cells are shown in Fig. 1(a), where the cell with the ITO nano-whisker ARC appears black compared to the conventional cell with blue color. The different reflective color is caused by the optical refection spectrum. Figure 1(b) and 1(c) show the cross-sectional and tilted top view scanning electron micrographs (SEM) of the evaporated ITO nano-whiskers on the micro-textured si solar cell, where the nano-whiskers are very uniformly distributed. In our experimental, we can deposited the ITO nano-whiskers to the maximum area of 10cm*10cm.

3. RESULT

Figure 2 shows the SEM images of ITO-whisker grown at various deposition times: (a)9 min., (b)18min.,(c) 27min, and (d) 36 min.. The ITO nanowhisker shows diameter in the range of 30nm to 50nm depends on the deposition time. The longer deposited time results in higher and denser ITO whiskers. The height of ITO whiskers is 330nm, 450nm, 750nm, 750nm for each condition, respectively. In our experimental, the height of the nanowhiskers would saturate at the height of 750nm, which depends on the deposition temperature. Moreover, the lower temperature can grow higher height of whiskers. Presumably, the ITO nano-whisker growth is facilitated by a self-catalyst vapor-liquid-solid (VLS) mechanism. In the past, the catalyst VLS mechanism is used for grow ITO nano-columns by metal catalyst, such as Sn nano-particle or Au. The catalyst induced a lower melting point near the interface causing neculi-crystal growth. In this case, the doped Sn atoms play the role of the catalyst that decreases the melting point of In-Sn alloy. The thin surface then turns into the

liquid phase due to the high Sn composition. The liquid phase promotes the absorption of the ITO vapor to supply In_2O_3 growth in various directions, resulting in the whisker structures.

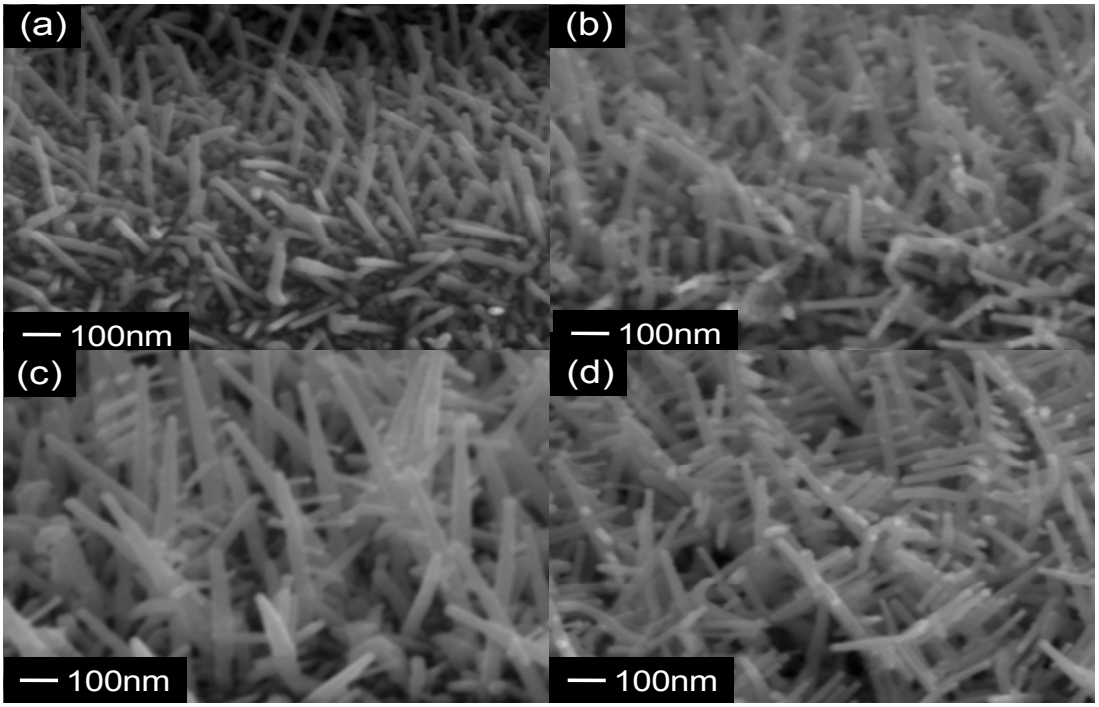

Figure 2 The ITO whisker structures grown with different deposited times: (a) 9min (b) 18min (c) 27min (d) 36min. The longer deposited time results in higher and denser ITO whiskers.

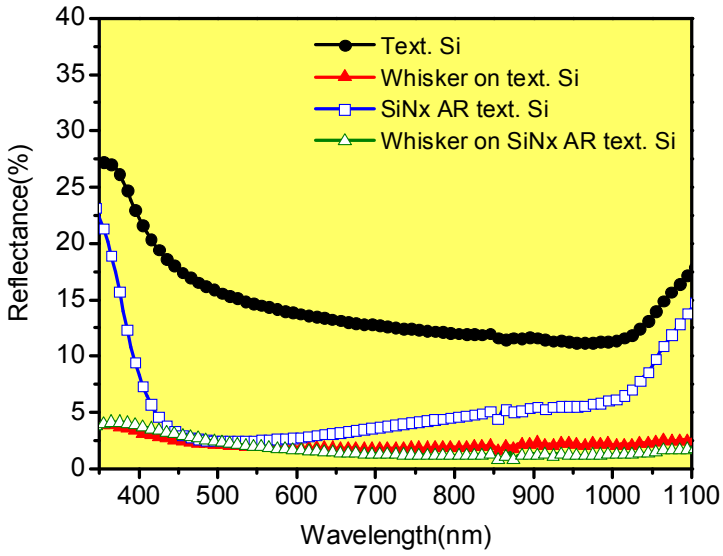

Figure 3 The comparison of the measured reflectence of surface-textured silicon solar cells with various AR coatings: no AR treatment, a SiN_x ARC, ITO nano-whisker AR layer deposited on a bare Si cell and on the SiN_x ARC.

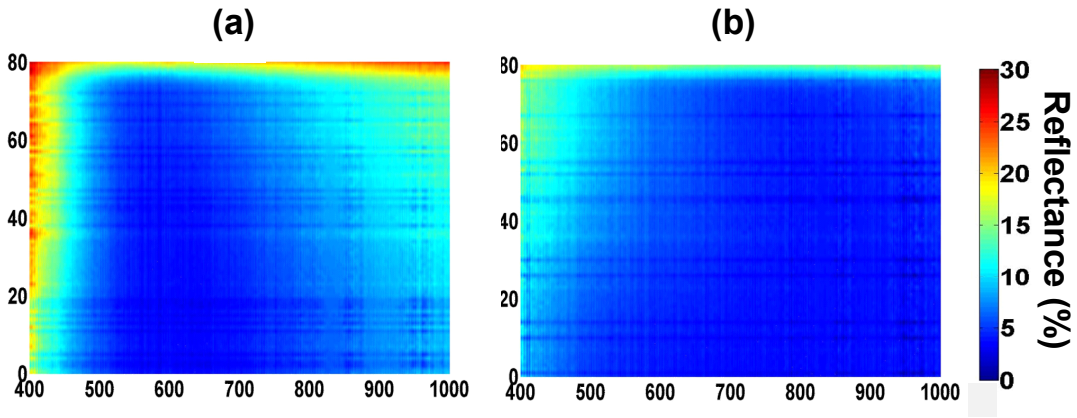

Figure 4 Angle-resolved reflectance spectra for (a) a conventional micro-grooved silicon substrate with an 80-nm-thick SiN_x antireflection coating, and (b) with both SiN_x and indium-tin-oxide nanowhiskers.

The reflectance spectroscopy was conducted in a UV-VIS spectrometer for Lambda 750 (PerKinElmer corp.), including an integral sphere with a light spot diameter of $1cm^2$. As shown in Fig. 3, the reflectance of cells with the ITO nano-whiskers exhibit broadband anti-reflective characteristics ($R < 5\%$) for the wavelength range of 350nm-1100nm. Compared to that of a textured Si substrate without any ARC and with a SiN_x ARC, ITO nano-whiskers successfully suppress the reflection in the near-infrared wavelength range from 700nm to 1100nm. The ITO nano-whisker layer functions as an optical buffer layer with low refractive indices to suppress the Fresnel reflection [9].

Figure 4(a) and 4(b) presents an angle-resolved reflectance spectroscopy for textured silicon substrates with the conventional antireflection coating and with optimized ITO nanowhiskers, respectively, up to an incident angle of 80° and a wavelength of 1000 nm. It can be clearly seen that the reflection at the near-infrared is detrimental for the conventional coating, and further deteriorates with the increase of incident angles. The high reflection at the near-infrared could further worsen the weak optical absorption in thin silicon wafers. In contrast, the combined micro- and nano-scale surface textures suppress optical reflection in the infrared wavelengths, as represented by the dark blue color on the right half plane of Figure 4(b). Still, the surface textures may also give rise to scattering and slightly raise the reflection by less than 1% between the 500 and 600 nm wavelengths at oblique incident angles between 40° and 75°.

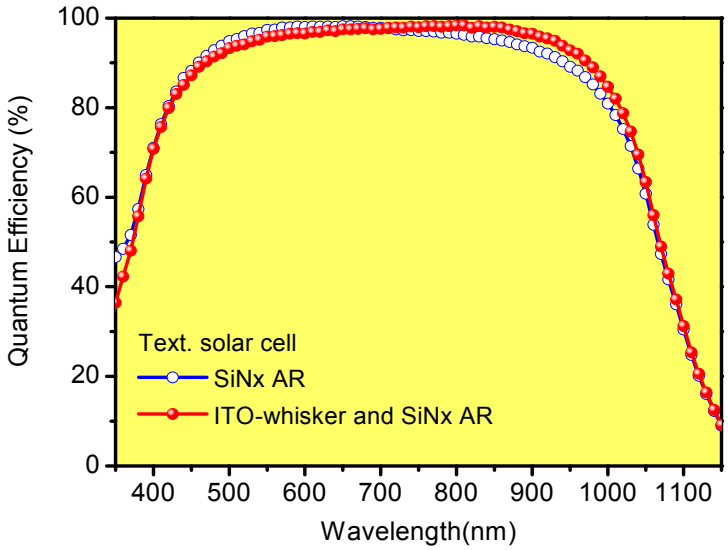

Fig. 5 The ITO-whiskers solar cell show an enhancement of quantum efficiency at the near infrared (NIR) wavelength region of 700~1100nm.

The external quantum efficiency (EQE) measurement of ITO-whisker cell and a reference cell with a 80nm thick SiN_x layer. As shown in Fig. 5, the quantum efficiency of the cell with whisker ARC reflects the enhancement in the wavelength range of 700-1000nm due to the improved light transmission. Moreover, the corresponding current-density-voltage characteristics are shown in Fig. 6(a). The short-circuit current density (Jsc) of the whisker cell increases by 1.41mA/cm^2, from 35.84mA/cm^2 to 37.36mA/cm^2. Overall, the PCE is also enhanced by 7% (from 16.08% to 17.18%) by using the ITO nano-whisker ARC. In addition, the angular response of the PCE is also enhanced by a factor of 7% at the normal incidence to more than 15% for incident angles over 70º, as shown in Fig. 6(b). Since the ITO nano-whisker ARC can enhance light transmittance at large incident angles, The angular responses of the short circuit current and open-circuit voltage also increase compared to conventional cells.

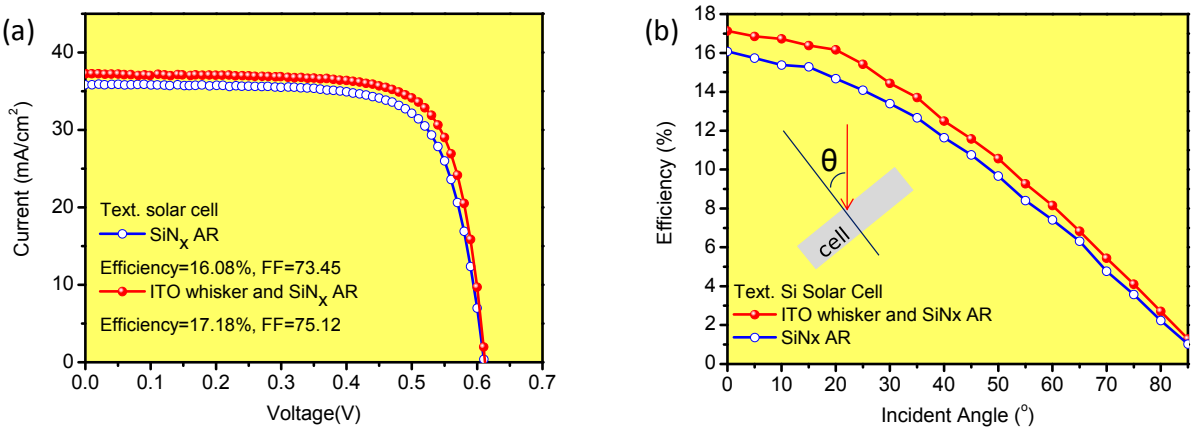

Figure 6 (a) The measured current-density-voltage characteristics for cells with nano-whisker ARC and conventional SiNx ARC. (b) The angular response of the PCE, which is enhanced by a factor of ~7% at the normal incidence to more than 15% for incident angles over 70º.

4. CONCLUSION

In conclusion, distinctive ITO nano-whiskers, grown by glancing-angle deposition, have been employed as a cost-effective ARC for Si solar cells. Reflectance spectroscopy verifies that the nanostructure exhibits excellent anti-reflection at normal incidence for the wavelength range of 350nm~1100nm. The nanostructured ITO AR layer achieves 17.1% conversion efficiency and an enhancement factor of 15% or incident angles over 70º, confirming the broadband and omnidirectional AR response.

ACKNOWLEDGEMENT

The authors thank Prof. H. C. Kuo at National Chiao-Tung University for facility support. This work is supported by the National Science Council in Taiwan under grant number, NSC 96-2221-E-009-092-MY3, NSC 97-2120-M-006-009 and the Bureau of Energy and Ministry of Economic Affairs in Taiwan.

REFERENCE

[1] Richards, B. S., "Comparison of TiO2 and Other Dielectric Coatings for Buriedcontact Solar Cells: a Review," Prog. Photovolt: Res. Appl. 12, 253-281 (2004).
[2] Martinet, C., Paillard, V., Gagnaire, A., and Joseph, J., "Deposition of SiO2 and TiO2 thin films by plasma enhanced chemical vapor deposition for antireflection coating," J. Non-Cryst. Solids 216, 77-82 (1997).

[3] Aroutiounian, V. M., Martirosyan, K., and Soukiassian, P., "Almost zero reflectance of a silicon oxynitride/porous silicon double layer antireflection coating for silicon photovoltaic cells," J. Phys. D: Appl. Phys. 39, 1623-1625 (2006).
[4] Clapham, P. B., and Hutley, M. C., "Reduction of lens reflexion by the 'moth eye' principle," Nature 244, 281-282 (1973).
[5] Wilson, S. J., and Hutley, M. C., "The optical properties of 'moth eye' antireflection surfaces," Opt. Acta 29, 993-1009 (1982).
[6] Lalanne, P., and Morris, G. M., "Antireflection behavior of silicon subwavelength periodic structures for visible light," Nanotechnology 8, 53-56 (1997).
[7] Srinivasarao, M., "Nano-optics in the biological world: Beetles, butterflies, birds, and moths," Chem. Rev. 99, 1935-1961 (1999).
[8] Chiu, M. Y., Chang, C. H., Tsai, M. A., Chang, F. Y., and Yu, P., "Improved optical transmission and current matching of a triple-junction solar cell utilizing sub-wavelength structures," Opt. Express 18, A308-A313 (2010).
[9] Huang, Y. F., Chattopadhyay, S., Jen, Y. J., Peng, C. Y., Liu, T. A., Hsu, Y. K., Pan, C. L., Lo, H. C., Hsu, C. H., Chang, Y. H., Lee, C. S., Chen K. H., and Chen L. C., "Improved broadband and quasi-omnidirectional anti-reflection properties with biomimetic silicon nanostructures," Nature Nanotech. 2, 770-774 (2007).
[10] Lee, Y. J., Ruby, D. S., Peters, D. W., McKenzie, B. B., and Hsu, J. W. P., "ZnO Nanostructures as Efficient Antireflection Layers in Solar Cells," Nano Lett. 8, 1501-1505 (2008).
[11] Boden, S. A., and Bagnall, D. M., "Tunable reflection minima of nanostructured antireflective surfaces," Appl. Phys. Lett. 93, 133108 (2008)
[12] Chang, C. H., Yu, P., and Yang, C. S., "Broadband and omnidirectional antireflection from conductive indium-tin-oxide nanocolumns prepared by glancing-angle deposition with nitrogen," Appl. Phys. Lett. 94, 051114 (2009).
[13] Yu, P., Chang, C. H., Chiu, C. H., Yang, C. S., Yu, J. C., Kuo, H. C., Hsu, S. H., and Chang, Y. C., "Efficiency Enhancement of GaAs Photovoltaics Employing Antireflective Indium Tin Oxide Nanocolumns," Adv. Mater. 21, 1618-1621 (2009).
[14] Peng, X. S., Meng, G. W., Wang, X. F., Wang, Y. W., Zhang, J., Liu, X., and Zhang, L. D., "Synthesis of oxygen-deficient indium-tin-oxide (ITO) nanofibers," Chem. Mater. 14, 4490-4493 (2002).
[15] Chen, Y. Q., Jiang, J., Wang, B., and Hou, J. G., "Synthesis of tin-doped indium oxide nanowires by self-catalytic VLS growth," J. Phys. D: Appl. Phys. 37, 3319-3322 (2004).
[16] Yumoto, H., Sako, T., Gotoh, Y., Nishiyama, K., Kaneko, T., "Growth mechanism of vapor-liquid-solid (VLS) grown indium tin oxide (ITO) whiskers along the substrate," J. Crystal Gowth, 203, 136-140 (1999).
[17] Takaki, S., Aoshima, Y., and Satoh, R., "Growth mechanisms of indium tin oxide whiskers prepared by sputtering", Jpn. J. Appl. Phys. 46, 3537-3544 (2007).